Ordinal Measures for Iris Recognition

Zhenan Sun, *Member*, *IEEE*, and Tieniu Tan, *Fellow*, *IEEE*

Abstract—Images of a human iris contain rich texture information useful for identity authentication. A key and still open issue in iris recognition is how best to represent such textural information using a compact set of features (iris features). In this paper, we propose using ordinal measures for iris feature representation with the objective of characterizing qualitative relationships between iris regions rather than precise measurements of iris image structures. Such a representation may lose some image-specific information, but it achieves a good trade-off between distinctiveness and robustness. We show that ordinal measures are intrinsic features of iris patterns and largely invariant to illumination changes. Moreover, compactness and low computational complexity of ordinal measures enable highly efficient iris recognition. Ordinal measures are a general concept useful for image analysis and many variants can be derived for ordinal feature extraction. In this paper, we develop multilobe differential filters to compute ordinal measures with flexible intralobe and interlobe parameters such as location, scale, orientation, and distance. Experimental results on three public iris image databases demonstrate the effectiveness of the proposed ordinal feature models.

Index Terms—Biometrics, feature representation, iris recognition, multilobe differential filter, ordinal measures.

1 Introduction

Iris recognition, as an extremely reliable method for identity authentication, is playing a more and more important role in many mission-critical applications, such as assess control, national ID card, border crossing, welfare distribution, missing children identification, etc. The uniqueness of iris pattern comes from the richness of texture details in iris images, such as freckles, coronas, crypts, furrows, etc. It is commonly believed that it is impossible to find two persons with identical iris patterns, even they are twins. The randomly distributed and irregularly shaped microstructures of iris patterns make the human iris one of the most informative biometric traits. On the other hand, the complex iris image structure results in the difficulty of iris feature representation. Although the human visual system can observe the distinguishing iris features effortlessly (see Fig. 1 for some example iris images), the computational characterization and comparison of such features is far from a trivial task and has attracted much attention for the past decade.

Daugman proposed the first successful algorithm for iris recognition [1]. In this algorithm, even and odd Gabor filters are proposed to demodulate phase information in each iris region. Then, phase value is coarsely quantized to 2-bit binary codes, and a given iris image is represented with 256 Bytes iris code. At the feature-matching step, the dissimilarity between two iris codes is measured by Hamming distance. Daugman's algorithm [1], [2] has been widely used in commercial iris recognition products. Wildes et al. [3] represented iris patterns using the four-level Laplacian pyramid and the goodness of matching was determined by the normalized correlation results between two registered iris images. Boles and Boashash [4] detected zero crossings of one-dimensional wavelet transform over concentric circles on the iris. Both the position and magnitude information of zero-crossing representations were used for matching. Ma et al. proposed describing iris features using texture analysis, based on a bank of spatial filters [5]. Regarding an iris image as a transient signal, Ma et al. [6] identified the local sharp variation points as iris features. Other iris representation methods include emergent frequency and instantaneous phase [7], local texture energy orientation [8], Haar wavelet frame decomposition [9], multiscale zero-crossing representation [10], normalized directional energy feature [11], Haar wavelet binary features [12], correlation filters [13], Gaussian-Hermite moments [14], local extreme points [15], discrete cosine transform [16], direction of gradient vector field [17], etc.

Great progress has been made on iris feature representation, but it is still an open problem. First, although there is a defined standard for raw iris data [42], there is none regarding iris features. A number of iris recognition methods [6], [7], [8], [9], [10], [15], [16], [17] have reported comparable performances to that of Daugman's algorithm [1], [2], but these methods encoded iris features from different perspectives. Second, recognition performance of the state-of-the-art iris features still has much room to be improved. Testing results of both International Biometrics Group ($\mathrm{FRR} =$ 2-5% @ $\mathrm{FAR} = 10^{-6}$) [18] and Iris Challenge Evaluation in 2006 ($\mathrm{FRR} =$ 1-3% @ $\mathrm{FAR} = 10^{-3}$) [19] demonstrate that the state-of-the-art iris recognition methods are far from perfect. A possible way to improve iris recognition performance is to explore more effective features for iris image representation.

The most challenging issue in iris feature representation is to achieve sensitivity to interclass differences and at the same time to maintain robustness against intraclass variations. So, a most important question one may ask is "What are the intrinsic and robust features of iris patterns?" or in practice, "How do we computationally

• *The authors are with the Center for Biometrics and Security Research, National Laboratory of Pattern Recognition, Institute of Automation, Chinese Academy of Sciences, No. 95, Zhongguancun East Road, Haidian District, PO Box 2728, Beijing 100190, PR China.*
E-mail: {znsun, tnt}@nlpr.ia.ac.cn.

Manuscript received 18 Feb. 2008; revised 25 Aug. 2008; accepted 2 Sept. 2008; published online 2 Oct. 2008.
Recommended for acceptance by S. Prabhakar.
For information on obtaining reprints of this article, please send e-mail to: tpami@computer.org, and reference IEEECS Log Number.
TPAMI-2008-02-0106.
Digital Object Identifier no. 10.1109/TPAMI.2008.240.

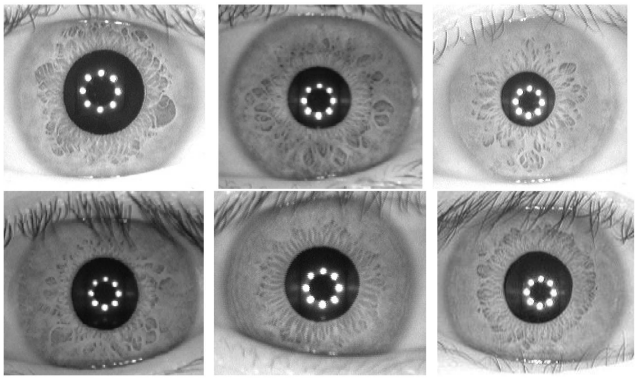

Fig. 1. Some iris images from the CASIA database [36].

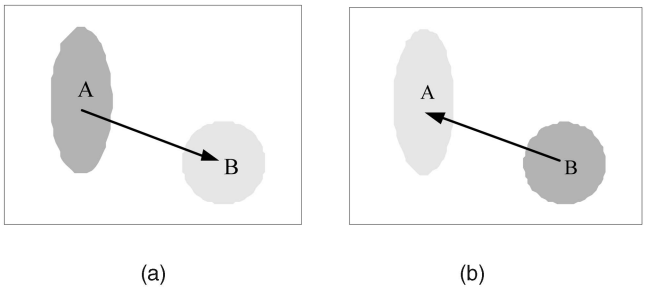

Fig. 2. Ordinal measure of relationship between two regions. An arrow points from the darker region to the brighter one. (a) Region A is darker than B, i.e., $A \prec B$. (b) Region A is brighter than B, i.e., $A \succ B$.

model iris texture effectively and efficiently?" An equally important question to ask is "Do the currently best performing iris recognition algorithms have anything in common and what makes them effective?" Many iris recognition methods [1], [2], [3], [4], [5], [6], [7], [8], [9], [10], [11], [12], [13], [14], [15], [16], [17] have been reported, but these questions remain open and intriguing.

In this paper, we introduce ordinal measures for iris image representation in an attempt to answer some of these questions. Ordinal measures encode qualitative information of visual signal rather than its quantitative values. Such an idea is motivated by findings in neuroscience [20]. For iris recognition, the absolute intensity information associated with an iris pattern can vary because it can change under different illumination settings. However, ordinal measures among neighboring image pixels or regions exhibit some stability with such changes and reflect the intrinsic properties of iris. In iris patterns, microstructures exhibit sharp intensity variations in iris images, which constitute numerous high contrast and stable ordinal relationships between iris regions. Therefore, ordinal measures are expected to be capable of representing the distinctive and robust features of iris patterns.

The remainder of this paper is organized as follows: Section 2 presents a brief introduction to ordinal measures and analyzes their important properties for iris image analysis. Section 3 proposes a novel ordinal feature extractor, namely, multilobe differential filter for iris recognition. In Section 4, feature representation models of existing iris recognition methods are discussed in the context of ordinal measures. Experimental results on three publicly available iris image databases are reported in Section 5. Section 6 concludes this paper. Preliminary results on ordinal measures in iris recognition were presented in [39], [40]. In passing, it should be pointed out that ordinal measures and ordinal features are interchangeable terms in this paper.

2 Ordinal Measures and Their Properties for Iris Image Analysis

2.1 A Brief Introduction to Ordinal Measures

Stevens suggested four levels of measurements from coarse to fine: nominal, ordinal, interval, and ratio measures [21]. Ordinal measures come from a simple and straightforward concept that we often use. For example, we can easily rank or order the heights or weights of two persons, but it is hard to tell their precise differences. This kind of qualitative measurement, which is related to the relative ordering of several quantities, is defined as ordinal measures (OMs).

A simple illustration of ordinal measures is shown in Fig. 2, where the symbol "$\prec$" or "$\succ$" denotes the inequality between the average intensities of two image regions. The inequality represents an ordinal relationship between two regions and this yields a symbolic representation of the relations. For digital encoding of the ordinal relationship, only a single bit is enough, e.g., "1" for "$A \prec B$" and "0" for "$A \succ B$," and the equality case (a low probability event) can be assigned to either.

Ordinal measures have been described [21] as a basic category of human perceptual judgments and widely used in social science. Ordinal measures also play an important role in nonparametric statistics. For example, rank statistic is proposed to measure the strength of the associations between two variables. Rank correlation methods have been widely used by statisticians, educators, psychologists, and others involved in analyzing qualitative measurements [22].

Computer vision researchers prefer interval or ratio measures for precise object feature description and pattern recognition. As the lowest level of measurement, nominal measures are actually too weak for pattern classification. But the power of ordinal measures for visual feature representation has been largely underestimated. We argue that ordinal image representation provides a better trade-off for computer vision systems between accuracy, robustness, and efficiency for the following reasons:

- The dominant image feature representation models in computer vision such as subspace analysis, statistics of image filter outputs, wavelet transform, etc., are based on high-level measurements. But the experiences of the last 40 years show that robustness is still the largest bottleneck of computer-based vision systems. The main reason is that interval or ratio measures of image contents are sensitive to illumination changes, blur, noise, deformation, and other image degradations. Fine models of visual objects based on high-level measurements are useful for image detail preservation and image reconstruction but unnecessary for object recognition. So, an innovative idea to robust representation of image features is to use ordinal measures.

- Real-time processing of visual signals is desirable for practical computer vision systems. However, the mathematical models of high-level measures are always complex and involve time-consuming computations. Since ordinal measures are simple to implement and compact in feature template, they are more suitable for efficient image analysis and pattern recognition than high-level measurements.
- The biological plausibility of visual ordinal measures has been verified by many neuroscience researchers [23], [24]. For example, DeAngelis et al. [23] found that many striate cortical neurons' visual responses saturate rapidly with the magnitude of contrast as the input. This indicates that the determining factor of visual perception is not the absolute value of contrast, but its polarity. Rullen and Thorpe [24] suggested that temporal order coding might form a rank-based image representation (i.e., ordinal measures) in the visual cortex.

The advantages of ordinal measures for visual representation have already been verified by some pioneering work in the literature. Sinha was probably the first to introduce ordinal measures to computer-based vision systems [25]. Based on the fact that several ordinal measures on facial images, such as eye-forehead and mouth-cheek, are invariant to individuals and imaging conditions, Sinha developed a ratio template for face detection, which can be automatically learned from examples [20], [25]. Combining qualitative spatial and photometric relationships together, Lipson et al. [26] applied ordinal measures to image database retrieval. Bhat and Nayar employed the rank permutation of pixel intensity values in image windows for stereocorrespondence [27]. After introducing ordinal measures into the co-occurrence model, Partio et al. obtained better texture retrieval results [28]. Smeraldi [29] proposed a complete family of multiscale rank features, namely, Ranklets, to describe the orientation-selective ordinal measures of image regions. Sadr et al. [30] developed a regularization approach for image reconstruction from ordinal measures.

Because of the simplicity of ordinal representation, Thoresz [31] believed that this scheme can only be used for simple detection and categorization tasks and did not expect it to be applied to complex discrimination tasks such as biometrics-based identity authentication.

However, we demonstrate in this paper that ordinal measures can play a defining role for the complex iris recognition task. Like any other pattern recognition problems, the key issue of iris feature representation is to handle the challenges from intraclass variations and interclass similarity. Some important intraclass variations of iris pattern that may affect the performance of iris recognition systems include illumination and contrast changes (Fig. 3a), occlusion of eyelids and eyelashes (Fig. 3b), nonlinear deformation (Fig. 3c), rotation difference (Fig. 3d, some methods can compute and correct the rotation angle between two iris images but alignment errors may exist), image degradations (Fig. 3e), intersensor difference (Fig. 3f), etc.

In conclusion, an effective iris feature representation model should be tolerant of the variations mentioned above and, at the same time, be capable of efficiently encoding the rich texture of iris images. Although this is a difficult problem, we will demonstrate in the following that ordinal measures provide a promising solution.

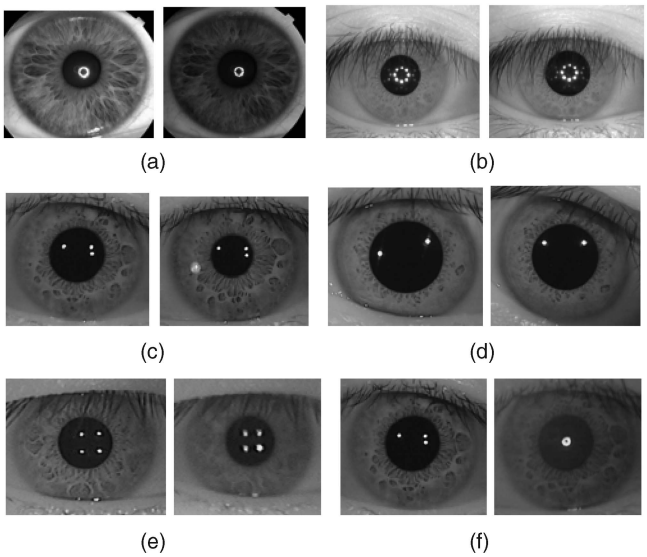

Fig. 3. Various intraclass variations of iris images. (a) Illumination and contrast variations. (b) Occlusions of eyelids and eyelashes. (c) Nonlinear deformation. (d) Rotation difference. (e) Image degradations. (f) Intersensor difference.

2.2 Desirable Properties of Ordinal Measures

The ordinal measures outlined above have a number of properties very desirable for accurate and robust iris recognition. This is briefly discussed in the following.

2.2.1 Robustness of Ordinal Measures

Formation of an iris image is jointly determined by both intrinsic factors (anatomical characteristics) and extrinsic factors (illumination, distance, position, rotation, etc.). Intrinsic factors are identity-related and stable for personal recognition, but extrinsic factors are independent of identity and variable under various imaging conditions. Iris image preprocessing methods can normalize part of extrinsic factors such as translation, scale, and rotation. We show in Appendix A that ordinal measures indicate intrinsic iris features and are largely invariant to illumination changes. A simple analysis of the robustness of ordinal measures against additive Gaussian noise is provided in Appendix B. Such a result can be extended to robustness of ordinal measures against dust on eyeglasses, partial occlusions, sensor noise, etc.

2.2.2 Uniqueness of Ordinal Measures

Iris pattern is a random texture characterized by many interlacing minute structures. The microanatomical structures in the iris surface may exhibit different reflectance properties in infrared light, leading to sharp intensity variations across iris image regions. The noise-like chaos may disturb the accuracy of traditional-segmentation-based computer vision algorithms. On the contrary, the numerous image region pairs with significant intensity difference provide abundant high-quality building blocks for ordinal template construction. We can imagine that the richness of

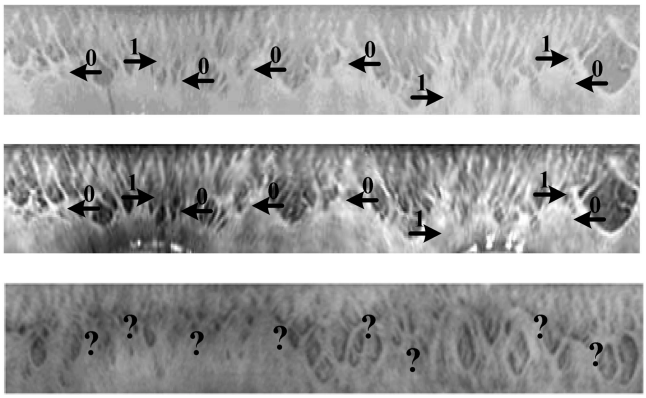

Fig. 4. Comparison of intraclass and interclass ordinal measures in normalized iris images. The upper two iris images are from the same eye and their ordinal measures are largely invariant even under different illuminations. However, the probability of matching interclass ordinal measures (e.g., corresponding regions between the lower two images) is only around 50 percent.

the uncorrelated ordinal measures is critical to the uniqueness of iris pattern. For an arbitrary pattern, its ordinal measure has equal probability to be "1" or "0." It is not difficult to find hundreds of independent ordinal measures in a typical iris image [1], [2], so a well-developed ordinal feature template of iris image should have at least hundreds of degrees-of-freedom for personal identification. Although the discriminating power of a single-bit ordinal measure is limited, the composite iris representation constituted by thousands of robust ordinal measures is powerful for large-scale personal identification.

Since ordinal measures are both robust and distinctive, they are ideal for feature representation. Fig. 4 illustrates the core idea of ordinal-measures-based iris recognition. Robustness contributes to high matching score of intraclass ordinal measures and distinctiveness guarantees dissimilarity between interclass ordinal measures. So, it is easy to distinguish genuine and imposter iris images based on the percentage of matched ordinal measures with the enrolled templates.

2.2.3 Efficiency of Ordinal Measures

A well-developed iris feature representation should reduce the computational complexity of feature extraction and feature matching to a minimum, which is beneficial to large-scale deployment and embedded applications of iris recognition. Ordinal feature extraction typically involves only additions and subtractions (e.g., the ordinal measure in Fig. 2 can be computed by sum(RegionA)-sum(RegionB)). This makes ordinal measures well suited for iris recognition on many weak computational platforms such as mobile phones and PDAs as they are not good at multiplications and divisions. The dissimilarity between two ordinal templates can be measured by bitwise XOR operator, which can be computed on-the-fly and can be easily implemented by hardware.

3 Ordinal Feature Extraction for Iris Recognition

In the preceding sections, we have discussed the basic concept of ordinal measures and their desirable properties

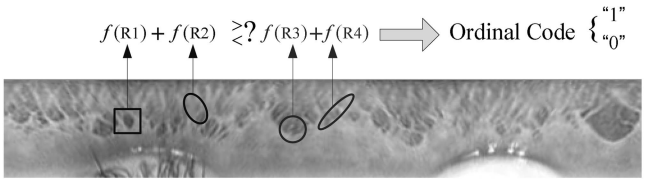

Fig. 5. Computing ordinal measures of iris images.

in the context of iris recognition. We now turn our attention to the issue of how to extract ordinal iris features.

Ordinal feature extraction of iris images is not a challenging issue due to the theoretical simplicity of ordinal measures. For example, an ordinal measure can be easily obtained by qualitatively comparing the features of two groups of image regions (see Fig. 5 for an example).

However, due attention should be paid to the selection of a number of intra and interregion parameters such as shape of regions, orientation of regions, location of regions, regional feature type (average intensity, wavelet coefficient, etc.), interregion distance, spatial configuration of regions, etc. These parameters lead to great flexibility in designing a particular scheme for ordinal iris feature extraction. In this sense, ordinal measures make it possible for us to develop a general framework for iris feature extraction. Specific feature extraction schemes can be derived from variations of these parameters.

In this paper, we propose multilobe differential filters (MLDFs) for ordinal iris feature extraction, aiming to model the flexibility of ordinal measures. Mathematically, the MLDFs are given as follows when Gaussian kernel is employed as the basic lobe:

$$MLDF = C_{\mathrm{p}} \sum_{i=1}^{N_{\mathrm{p}}} \frac{1}{\sqrt{2\pi}\delta_{\mathrm{p}i}} \exp\left[\frac{-(X-\mu_{\mathrm{p}i})^2}{2\delta_{\mathrm{p}i}^2}\right] - C_{\mathrm{n}} \sum_{j=1}^{N_{\mathrm{n}}} \frac{1}{\sqrt{2\pi}\delta_{\mathrm{n}j}} \exp\left[\frac{-(X-\mu_{\mathrm{n}j})^2}{2\delta_{\mathrm{n}j}^2}\right], \quad (1)$$

where the variables μ and δ denote the central position and the scale of a 2D Gaussian filter, respectively, N_{p} the number of positive lobes, and N_{n} the number of negative lobes. Constant coefficients C_{p} and C_{n} are used to ensure zero sum of the MLDF, i.e., $C_{\mathrm{p}}N_{\mathrm{p}} = C_{\mathrm{n}}N_{\mathrm{n}}$. The most compelling feature of MLDF compared with traditional differential filters is that it decouples the settings of intralobe (scale) and interlobe (distance) parameters. So, multilobe differential filters can be used to encode ordinal measures of both connected and dissociated image regions. Young et al. have already proposed difference-of-offset-Gaussians (DOOG) filter as the spatiotemporal model in visual neuroscience [34], which is similar to MLDF. DOOG is defined as the offset differences of two or more Gaussian functions. Higher order DOOG is created by additional offset differencing of lower order DOOG filters [34]. Compared with DOOG, MLDF is a more general concept of differential and bandpass filters and is more flexible in terms of basic lobe choice, spatial configuration of lobes, etc. Different from the dissociated dipole proposed by Balas and Sinha [32], [33], MLDF is constituted by more basic lobes and the shape of each lobe can be adaptive to image

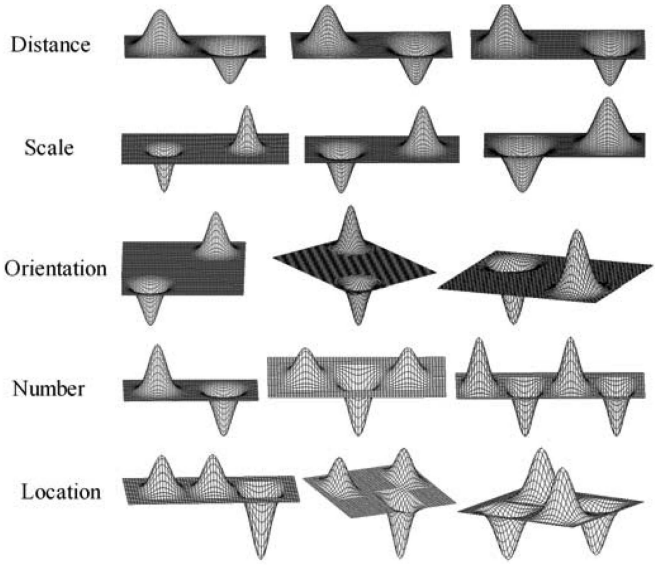

Fig. 6. Some examples of multilobe differential filters.

structures. The motivation is straightforward. When more than two image regions are compared, the derived ordinal measure is expected to be more robust. In addition, an ordinal measure extracted by MLDF can represent more complex image microstructures. Comparatively, a dissociated dipole can only tell us a slope edge's orientation. Some examples of MLDF with different settings of distance, scale, orientation, number, and location are illustrated in Fig. 6.

Each ordinal measure may have its unique visual meaning. For example, as Fig. 7 shows, a group of two-lobe ordinal measures may denote point, line, edge, corner, ridge, slope, etc.

The procedure of iris feature extraction using MLDF is as follows: An MLDF operator slides across the whole normalized iris image and each ordinal comparison is encoded as one bit, i.e., 1 or 0 according to the sign of the filtering result. All of the binary iris codes constitute a composite feature of the input iris image, namely, ordinal code (OC). The dissimilarity between two iris images is determined by the Hamming distance of their features. In order to cope with the possible rotation difference between

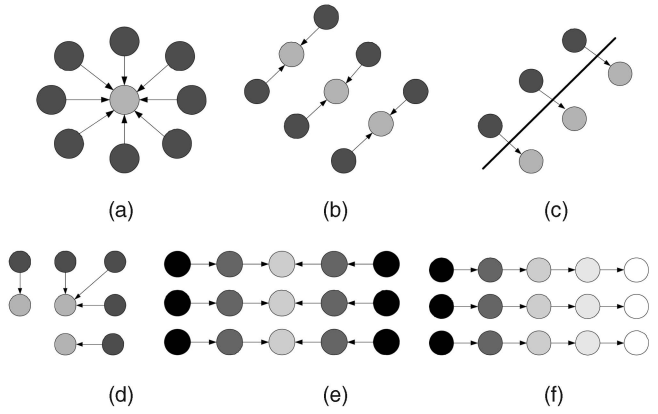

Fig. 7. Ordinal measures and their visual meanings. (a) Point. (b) Line. (c) Edge. (d) Corner. (e) Ridge. (f) Slope.

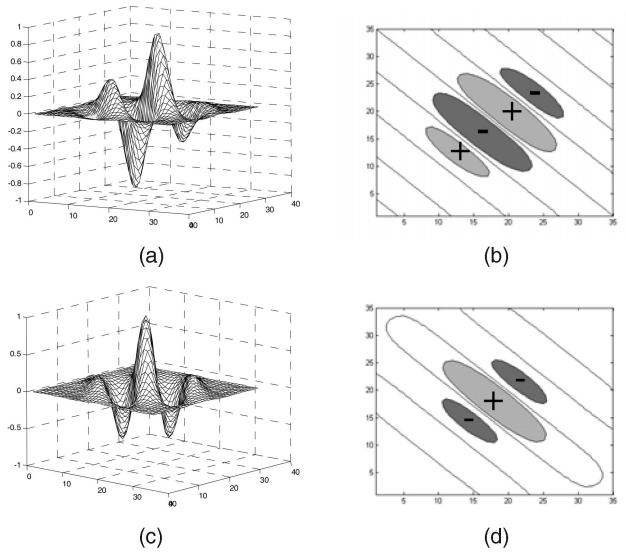

Fig. 8. Odd and even Gabor filters used in [1], [2]. (a) Odd Gabor filter. (b) Ordinal comparison of image regions using odd Gabor filter, where "+" denotes image region covered by excitatory lobe and "−" represents image region covered by inhibitory lobe. (c) Even Gabor filter. (d) Ordinal comparison of image regions using even Gabor filter.

the two iris images, the input ordinal code is circularly rotated at different starting angles to match the template ordinal code. And the minimum Hamming distance of all matching results is the measure describing the dissimilarity between the two iris images. Because iris localization and normalization have complemented the position and scale differences between two iris images, the whole procedure of iris matching is insensitive to position, scale, and rotation changes.

In summary, iris features based on ordinal comparisons represent iris image contents at three levels of scales: each iris feature element (ordinal code) describes the ordinal information of an image patch covered by the MLDF which is localized by the central *pixel* of the image patch; each ordinal measure is jointly determined by weighted intensities of several *regions*; and finally, all ordinal measures are concatenated to build a *global* description of the iris image.

4 Existing Iris Recognition Algorithms in the Context of Ordinal Measures

Based on ordinal measures, we can provide a general framework for iris feature representation and extraction. Specific iris coding schemes can be obtained under the guidance of this framework by changing parameter configurations. Furthermore, with the above OM representation model in place, we show in the following that iris image features of a number of best-performing iris recognition methods may be interpreted as special cases of this model.

Gabor-based encoding filters used in iris code [1], [2] are essentially ordinal operators (see Fig. 8). Gabor filters by definition are continuous functions and have numerous lobes, but only a very small number of main lobes really matter. For odd Gabor filtering of local image patch, the image regions covered by two excitatory lobes are compared with the image regions covered by two inhibitory lobes (Fig. 8b). The filtered result is qualitatively encoded as

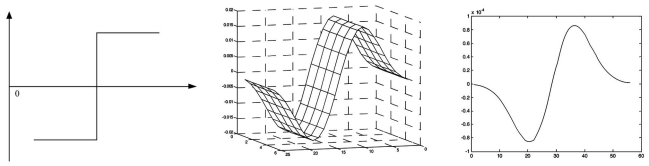

(a) (b) (c)

Fig. 9. Other special ordinal filters used for iris recognition. (a) Haar wavelet. (b) Quadratic spline wavelet. (c) The derivative of Gaussian.

"1" or "0" based on the sign of this inequality. Similarly, even Gabor-generated iris code is mainly determined by the ordinal relationship between one excitatory lobe-covered region and two small inhibitory lobes-covered regions (Fig. 8d). Because the sum of the original even Gabor filter's coefficients is not equal to 0, the average coefficient value is subtracted from the filter to keep the balance between positive coefficients and negative coefficients. Thus, each iris code has approximately equal probability of being "1" or "0" to maximize the randomness of iris features [1], [2].

Similarly, the Haar wavelet [9], quadratic spline wavelet [6], [10], and the derivative of Gaussian filter [15] may also be seen as typical ordinal filters (Fig. 9). The encoding methods of [9], [10], [15] are based on the sign representation of ordinal filtering results. Ma et al. [6] used the wavelet transform results as the measurements for ordinal comparison and a magnitude threshold was used to suppress the insignificant ordinal measures. Monro et al. proposed to compare the power spectrum of two iris image patches for ordinal encoding [16]. These iris recognition methods [1], [6], [9], [10], [15], [16] all perform well in large scale testing.

Although the connection between the state-of-the-art iris recognition methods and ordinal measures is only qualitatively established, our findings may help to explain these originally different and complex algorithms using a single framework (the OM framework), and provide a general iris feature exchange format based on ordinal measures. More importantly, such a framework is beneficial to guide further development of advanced iris feature representations. Because the difference in accuracy between the state-of-the-art iris recognition methods mainly comes from the different ordinal features they employed for recognition, our future work will focus on the selection of the optimal ordinal features.

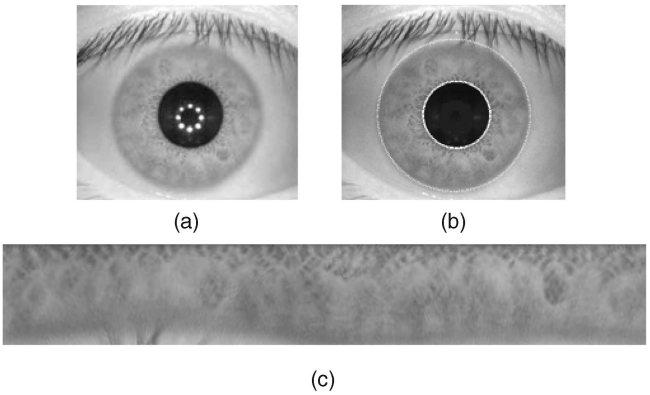

(a) (b) (c)

Fig. 10. Illustration of iris image preprocessing. (a) Original iris image. (b) Iris localization (specular reflections in the pupil region are automatically detected and filled with low-intensity pixels). (c) Iris normalization.

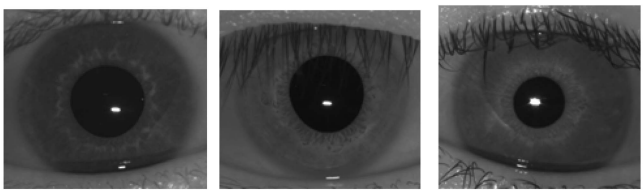

Fig. 11. ROI of the sample iris images in the UBath database [35].

5 Experimental Results

Extensive experiments have been conducted to evaluate the performance of the proposed ordinal measures for iris recognition. Three iris image databases, namely, UBath [35], CASIA [36], and ICE2005 [19], are used as the test data sets. These databases represent the most challenging data set for iris recognition currently available in the public domain. The Gabor phase encoding method (iris code) [1], [2], which is the most successful iris recognition algorithm in commercial applications, and local sharp variation method (shape code) [6], which achieved high performance in both accuracy and speed simultaneously, are implemented by ourselves as the benchmark algorithms in this paper.

Before iris image feature extraction using different encoding algorithms, the original iris image must be preprocessed. It mainly includes iris localization and normalization (see Fig. 10).

Since the focus of this paper is on iris feature representation, details of iris image preprocessing are not reviewed here but may be found in the literature [1], [3], [5], [6].

5.1 Results on the UBath Iris Image Database

The UBath Database [35] includes 8,000 iris images of 200 people (see Fig. 11 for some example images). The database is constructed with a machine vision camera under NIR illumination. Because of controlled capture interface, illumination, and cooperative volunteers, the quality of iris images in this database is good. The original image resolution is $1{,}280 \times 960$. To reduce computational costs, only the downsampled images (resolution 640×480) are used in this paper.

Two kinds of typical and simple ordinal filters (Fig. 12) with different configurations (in terms of the number of lobes and the interlobe distance) are used on the UBath

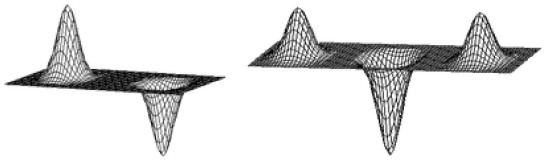

(a) (b)

Fig. 12. Two kinds of multilobe differential filters. (a) Dilobe ordinal filter. (b) Trilobe ordinal filter.

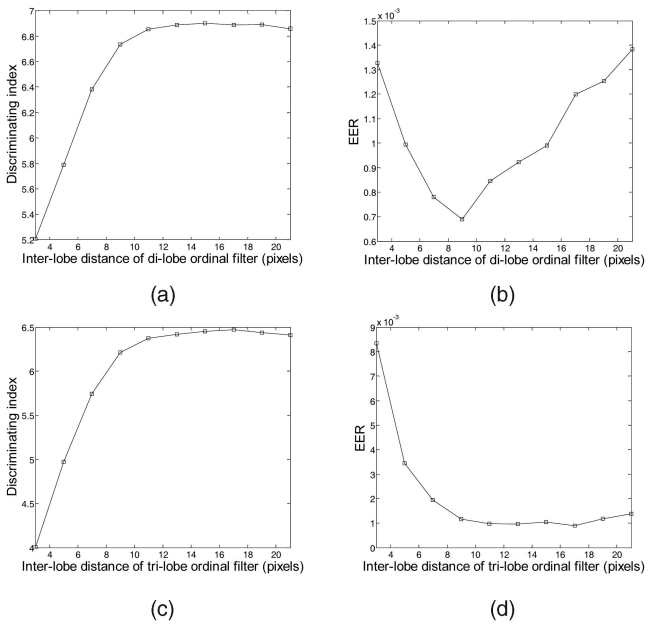

Fig. 13. Performance of ordinal filter as a function of interlobe distance on the UBath database. (a) DI of dilobe ordinal filter. (b) EER of dilobe ordinal filter. (c) DI of trilobe ordinal filter. (d) EER of trilobe ordinal filter.

database. The basic lobes of these filters are the same Gaussian filter (size is 5×5 and σ is 1.7). All the basic lobes are arranged horizontally to be comparable with previous schemes [2], [5], [6].

Each ordinal filter (dilobe or trilobe, with a variable interlobe distance ranging from 3 to 21) is performed on 1,024 densely sampled image regions, to obtain 128 bytes ordinal code for every iris image in the UBath database. Then, all possible intraclass comparisons (totally 76,022) are made to estimate the genuine distribution. To measure the imposter distribution, each image of one class is used to match all iris images with the same index in other classes, generating 1,595,978 interclass matching results (Note: The ground truth errors of class labels in the original UBath database have been corrected). Given the intra and interclass iris matching results, the recognition performance of every single ordinal filter is measured by the following two common indicators:

1. Equal error rate (EER), i.e., the cross-over error rate when false accept rate is equal to the false reject rate. Lower EER means higher accuracy of a biometric matcher.
2. Discriminating index d'(DI) [37], with the following definition:

$$d' = \frac{|m_1 - m_2|}{\sqrt{(\delta_1^2 + \delta_2^2)/2}}, \tag{2}$$

where m_1 and δ_1^2 denote the mean and variance of intraclass Hamming distances, and m_2 and δ_2^2 denote the mean and variance of interclass Hamming distances. Higher DI denotes higher discriminability of a biometric system.

Performance of ordinal filters measured by the above two indicators is shown in Fig. 13 with varying interlobe distances (d). From the experimental results, we can see that increasing interlobe distance improves recognition performance significantly, with lower EER and higher DI.

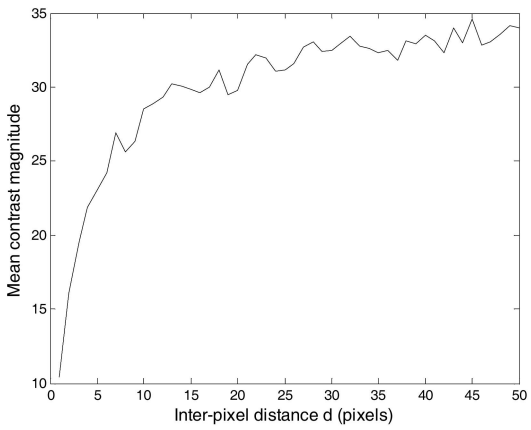

Fig. 14. The mean contrast magnitude as a function of the interpixel distance.

Here, we give a brief explanation of the advantages of increasing interlobe distance of ordinal measures. Because adjacent iris image regions are highly correlated to each other, the probability of two distant regions being different is much greater than that of two adjacent regions. For a typical iris image, the mean contrast magnitude of randomly sampled 1,000 pixel pairs as a function of the interpixel distance is shown in Fig. 14. From Fig. 14, it is obvious that the mean contrast magnitude is a monotonic increasing function of the interlobe distance. Of course, the contrast magnitude saturates when the interpixel distance is higher than a threshold, i.e., the two image pixels involved in ordinal comparison is completely uncorrelated. As discussed in Appendix B, the larger the contrast magnitude, the more robust the contrast polarity (ordinal measure). So, long-distance ordinal comparisons are more tolerant to common image degradations than purely local ones.

However, it is interesting to note that increasing interlobe distance does not always contribute positively to system performance (see Fig. 13b). We think that there may be two disadvantages of long-distance ordinal filter.

- When the overall kernel size of an ordinal filter becomes larger with the increasing of interlobe distance, more ordinal features are occluded by the eyelids and eyelashes due to the limited area of effective iris regions (Fig. 15). So, the number of valid feature codes in iris template decreases when the basic lobes of ordinal filter are further separated from each other, which is negative to recognition performance.
- Ordinal measures computed from too distant image regions lose the locality property and are easily affected by nonuniform illuminations, violating the basic assumption of ordinal feature extraction (Appendix A).

Considering that separating the basic lobes of an ordinal filter far from each other has its advantages and disadvantages, the trade-off is that an intermediate interlobe distance should be used for ordinal feature representation.

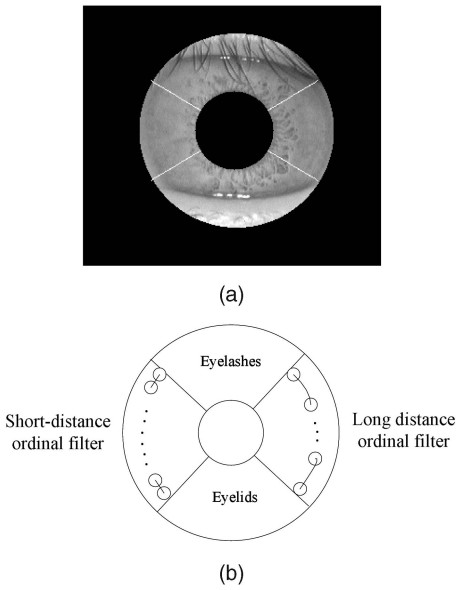

Fig. 15. Explanation of the disadvantage of ordinal measures between distant image regions.

Experimental results (Fig. 13b) show that, when the interlobe distance is about twice the diameter of the basic lobe, optimal recognition performance is achieved.

Since different ordinal filters have their specific characteristics, it is interesting to investigate the benefit of integrating multiple ordinal filters for iris recognition. As an example, we study two kinds of information fusion strategies, namely, fusion of dilobe and trilobe ordinal filters at score-level based on Sum rule, and fusion of neighboring (local) and dissociated (nonlocal) ordinal filters at score-level based on Sum rule.

Here, different performance indicators including EER, DI, Template size, and Computational cost of iris recognition algorithms with various parameter settings in ordinal filter are summarized in Table 1. Here, the computational cost means the time used for feature extraction, i.e., create one iris template from a normalized iris image. It is obvious that significant improvements of EER can be achieved by combining multiple ordinal filters. Both the iris code [1], [2] and the shape code [6] are tested on the same environment and compared with the local and nonlocal ordinal code (Table 1). ROC curves of iris recognition algorithms along with the confidence interval (CI) curve of FRR are shown in Fig. 16.

Compared with millions of interclass comparisons, the number of intraclass matchings is too small to achieve precise FRR estimation. Instead of point estimation, the confidence interval of FRR is more convincing to illustrate an algorithm's performance. FRR in ROC curve can be statistically estimated using bootstrap. Our experimental method based on the subsets bootstrap [38] is implemented as follows:

1. Obtain the Hamming distances of all intraclass and interclass iris image matching pairs.
2. Compute the thresholds $\{t_1, t_2, \ldots, t_{13}\}$ corresponding to logarithmically spaced FARs ranging from 10^{-6} to 10^{-2} (biometric system is often operated in this interval) based on the interclass Hamming distances.

TABLE 1
Comparison of Recognition Performance on the UBath Iris Database

Method	EER	DI	Template (Bytes)	Time (ms)
Di-lobe OC (d=5)	9.93×10^{-4}	5.79	128	5.2
Di-lobe OC (d=9)	6.88×10^{-4}	6.73	128	5.2
Di-lobe OC (d=5 plus d=9)	5.69×10^{-4}	6.34	256	10.4
Tri-lobe OC (d=5)	3.44×10^{-3}	4.97	128	5.2
Tri-lobe OC (d=17)	8.87×10^{-4}	6.47	128	5.2
Tri-lobe OC (d=5 plus d=17)	4.62×10^{-4}	5.91	256	10.4
Local OC (Di-lobe d=5 plus Tri-lobe d=5)	8.46×10^{-4}	5.43	256	10.4
Non-local OC (Di-lobe d=9 plus Tri-lobe d=17)	4.39×10^{-4}	6.72	256	10.4
Iris code [1]	1.24×10^{-3}	5.17	256	35.2
Shape code [6]	7.92×10^{-4}	6.28	256	29.6

3. Rewrite the N intraclass Hamming distances X as

$$X = \{x_1^1, x_1^2, \ldots, x_1^{y1}; x_2^1, x_2^2, \ldots, x_2^{y2}; \ldots; x_n^1, x_n^2, \ldots, x_n^{yn}\} = (\chi_1, \chi_2, \ldots, \chi_n), \quad (3)$$

where x_i^j denotes the jth intraclass Hamming distance of the ith class iris images, yi denotes the total number of intraclass comparisons in the ith class, and χ_i denotes the set containing all intraclass Hamming distances of the ith class.

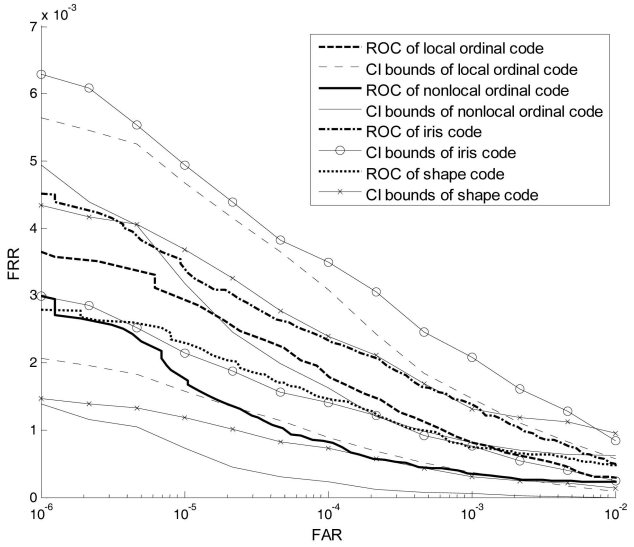

Fig. 16. ROC curves of iris recognition algorithms on the UBath database.

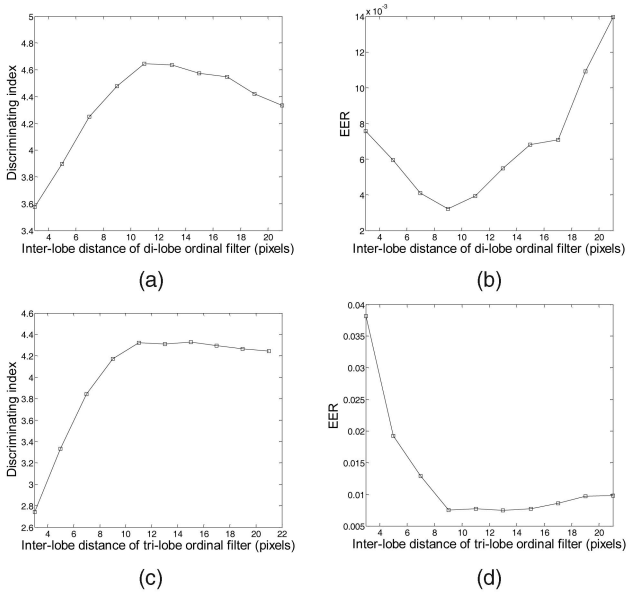

Fig. 17. Performance of ordinal filter as a function of interlobe distance on CASIA V1.0 database. (a) DI of dilobe ordinal filter. (b) EER of dilobe ordinal filter. (c) DI of trilobe ordinal filter. (d) EER of trilobe ordinal filter.

4. Create a bootstrap sample $X^* = \{\chi_1^*, \chi_2^*, \cdots, \chi_n^*\}$ by resampling n subsets χ with replacement from set X.
5. Calculate $F\hat{R}R_1(t_1), F\hat{R}R_2(t_2), \cdots, F\hat{R}R_{13}(t_{13})$ from X^*.
6. Repeat steps 4-5 20,000 times, resulting in 20,000 different estimates of FRRs denoted as $F\hat{R}R_1^K(t_1^*)$, $F\hat{R}R_2^K(t_2^*), \cdots, F\hat{R}R_{13}^K(t_{13}^*)$, $K = 1, 2, \cdots, 20{,}000$.
7. Estimate the 95 percent confidence interval of each FRR by the percentile method.

From the results in Fig. 16 and Table 1, we can see that all iris recognition algorithms perform well and are with overlapping confidence intervals. Accuracy of iris code, shape code, and ordinal code is comparable since there are totally 2,048 ordinal measures used in these methods, which are powerful enough to recognize successfully almost all iris images in the test set. However, there still exist some differences in the reported ROC curves of these four methods due to the different ordinal filtering strategies employed in feature extraction. Because even Gabor filter can be seen as a trilobe local ordinal filter (Fig. 8d) and odd Gabor filter can be seen as a quadlobe local ordinal filter (Fig. 8b), iris code performs like local ordinal code. Similarly, shape code's performance is also on the level of local ordinal code. It is demonstrated that suitable nonlocal ordinal code achieves better recognition performance than local one (see Table 1 and Fig. 16). Therefore, a possible way to improve state-of-the-art iris recognition performance is to break the limitation in local image filter configuration and introduce nonlocal ordinal measures for iris feature representation.

The time used for the computation of 256 bytes ordinal code using Matlab 7.0 on a Pentium IV 3.2 GHz processor with 1 GB RAM is 10.4 ms, but iris code needs 35.2 ms and shape code takes 29.6 ms under the same conditions (see Table 1). Ordinal code is more efficient than iris code and shape code because ordinal code generation only involves simple low-pass filtering and qualitative comparison. In contrast, iris code and shape code involve image filtering with complex Gabor and wavelet kernels, respectively.

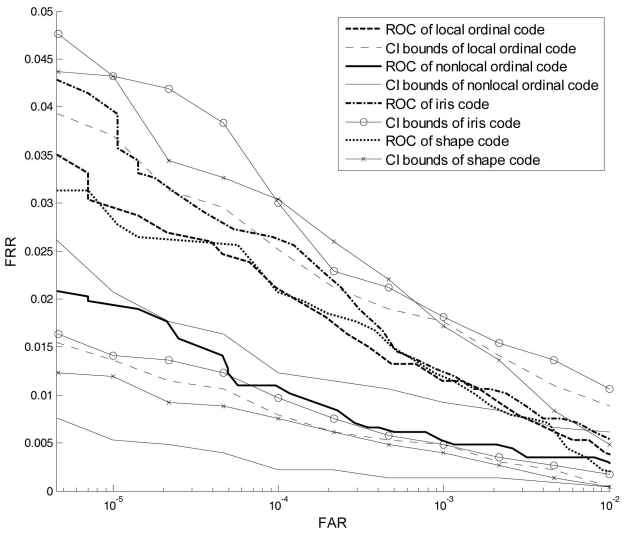

Fig. 18. ROC curves of iris recognition algorithms on CASIA V1.0 database.

5.2 Results on the CASIA Iris Image Database

CASIA Iris Image Database developed by our research group has been released to the international biometrics community for many years and has been considered as a standard database for the evaluation of iris recognition algorithms [36]. An earlier version of this database, CASIA Iris Database Ver 1.0 (CASIA V1.0), has been widely used in the literature, and it is also employed here as a benchmark to facilitate comparison between our results and others. Iris images of CASIA V1.0 were captured with a homemade iris camera. CASIA V1.0 contains 756 iris images from 108 subjects. In order to protect our IPR in the design of the iris camera (especially the NIR illumination scheme) before appropriate patents were granted, the pupil regions of all iris images in CASIA V1.0 were automatically detected and replaced with a circular region of constant intensity to mask out the specular reflections from the NIR illuminators before public release. Clearly, such processing may affect pupil detection but has basically no effects on other components of an iris recognition system such as iris feature extraction since iris feature extraction only uses the image data in the region between the pupil and the sclera, i.e., the ring-shaped iris region. All possible intra and interclass iris matchings are performed on CASIA V1.0 and the experimental results are shown in Figs. 17 and 18 and Table 2.

We note that Phillips et al. recently made some comments about CASIA V1.0 [41]. They stated the fact that the images in CASIA V1.0 had been preprocessed to have circular pupil regions of constant intensity before public release. They then recommend that "reporting experimental results on the CASIA Version 1.0 data set be discontinued, unless there is a compelling scientific reason to use it." As the preprocessing affects only the pupil region and iris feature extraction uses only iris data in the ring-shaped iris region which is not affected by the preprocessing, CASIA V1.0 is perfectly fine for the evaluation of iris feature extraction algorithms such as in this paper and [5]. Therefore, we think that their recommendations and comments about CASIA V1.0 are overstated and may lead to confusion and misunderstanding.

In addition to CASIA V1.0, the latest version of the CASIA database, CASIA-IrisV3, is also used in this paper

TABLE 2
Comparison of Recognition Performance on CASIA V1.0 Database

Method	EER	DI	Template (Bytes)	Time (ms)
Di-lobe OC (d=5)	5.94×10^{-3}	3.90	128	5.2
Di-lobe OC (d=9)	3.20×10^{-3}	4.48	128	5.2
Di-lobe OC (d=5 plus d=9)	2.28×10^{-3}	4.26	256	10.4
Tri-lobe OC (d=5)	1.92×10^{-2}	3.33	128	5.2
Tri-lobe OC (d=9)	7.47×10^{-3}	4.17	128	5.2
Tri-lobe OC (d=5 plus d=9)	4.68×10^{-3}	3.84	256	10.4
Local OC (Di-lobe d=5 plus Tri-lobe d=5)	5.65×10^{-3}	3.66	256	10.4
Non-local OC (Di-lobe d=9 plus Tri-lobe d=9)	3.70×10^{-3}	4.39	256	10.4
Iris code [1]	6.76×10^{-3}	3.73	256	35.2
Shape code [6]	5.01×10^{-3}	3.87	256	29.6

for testing. In particular, one of CASIA-IrisV3's three subsets, namely, CASIA-IrisV3-Interval, is used for evaluation in this paper. There are totally 2,655 iris images in this subset, acquired from 396 eyes of 249 subjects. Most volunteers of CASIA database are Chinese and most images were captured in two sessions, with at least one-month interval. All possible intra- and interclass iris matchings are performed on CASIA-IrisV3-Interval and the experimental results are shown in Figs. 19 and 20 and Table 3.

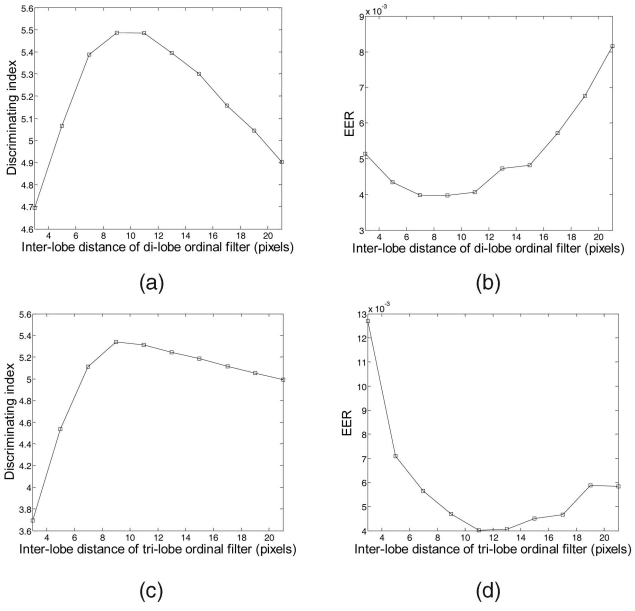

Fig. 19. Performance of ordinal filter as a function of interlobe distance on CASIA-IrisV3-Interval database. (a) DI of dilobe ordinal filter. (b) EER of dilobe ordinal filter. (c) DI of trilobe ordinal filter. (d) EER of trilobe ordinal filter.

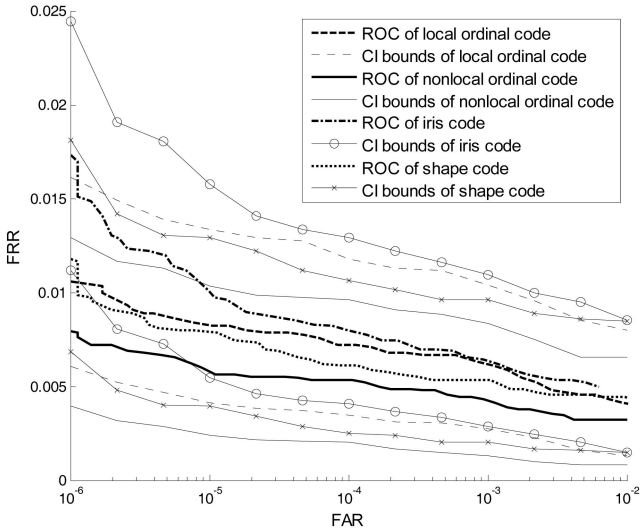

Fig. 20. ROC curves of iris recognition algorithms on CASIA-IrisV3-Interval database.

5.3 Results on the ICE2005 Iris Image Database

Iris Challenge Evaluation is organized by NIST and the first evaluation held in 2005 has released the data, protocol, and ground truth to participants [19]. The iris images of ICE2005 database were collected using LG2200 sensor, including 1,528 images of 120 left eyes and 1,425 images of 124 right eyes (see Fig. 21 for two example iris images). The data set was constructed in weekly acquisition sessions and contains iris images of different quality. To be compliant with the ICE2005 protocol [19], the iris recognition algorithms are separately evaluated on the left- and right-eye subsets, respectively.

TABLE 3
Comparison of Recognition Performance on CASIA-IrisV3-Interval Iris Database

Method	EER	DI	Template (Bytes)	Time (ms)
Di-lobe OC (d=5)	4.34×10^{-3}	5.07	128	5.2
Di-lobe OC (d=9)	3.97×10^{-3}	5.49	128	5.2
Di-lobe OC (d=5 plus d=9)	3.64×10^{-3}	5.39	256	10.4
Tri-lobe OC (d=5)	7.10×10^{-3}	4.53	128	5.2
Tri-lobe OC (d=11)	4.00×10^{-3}	5.31	128	5.2
Tri-lobe OC (d=5 plus d=11)	3.95×10^{-3}	5.12	256	10.4
Local OC (Di-lobe d=5 plus Tri-lobe d=5)	4.61×10^{-3}	4.89	256	10.4
Non-local OC (Di-lobe d=9 plus Tri-lobe d=11)	3.48×10^{-3}	5.50	256	10.4
Iris code [1]	5.15×10^{-3}	4.65	256	35.2
Shape code [6]	4.42×10^{-3}	5.12	256	29.6

Fig. 21. Example iris images of ICE2005 database.

5.3.1 Performance on Left-Eye Subset

All possible intra and interclass iris matchings are performed on ICE2005-Left iris database and the experimental results are shown in Figs. 22 and 23 and Table 4.

5.3.2 Performance on Right-Eye Subset

All possible intra and interclass iris matchings are performed on ICE2005-Right iris database and the experimental results are shown in Figs. 24 and 25 and Table 5.

5.3.3 Multiscale Ordinal Measures

The ordinal measures discussed above are all implemented at one scale (lobe size $5 \times 5, \sigma$ is 1.7). However, it is well accepted that iris texture details are exhibited in multiscale space [1], [3]. So, ordinal measures with different lobe size (5×5 and 9×9) are integrated together to build a more powerful iris feature model. Experimental results in Fig. 26 and Tables 4 and 5 demonstrate that the performance of multiscale ordinal measures is comparable to that of the top algorithms (Daugman's new methods, Sagem, CMU, Iritech) reported in the ICE2005 evaluation [19]. It should be noted that in this paper, no efforts have been made to optimize the ordinal code. Nevertheless, the recognition results demonstrate that ordinal measures are promising for iris feature representation. Moreover, it is possible to develop more advanced iris recognition engines by exploring the huge feature space of ordinal measures.

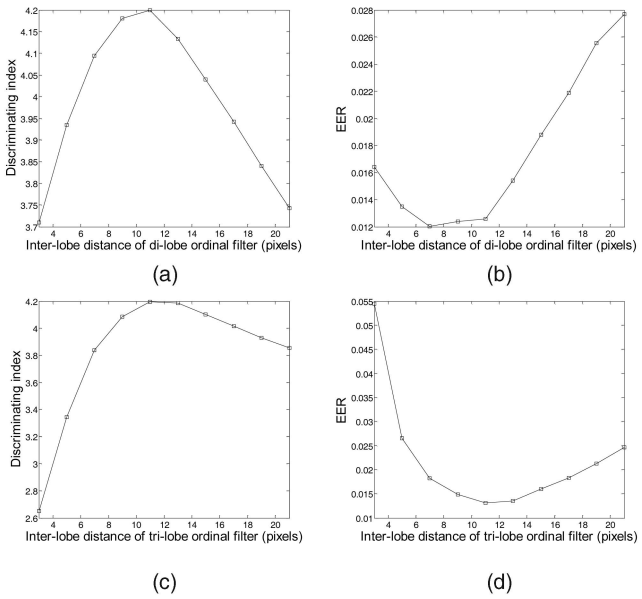

Fig. 22. Performance of ordinal filter as a function of interlobe distance on ICE2005-Left database. (a) DI of dilobe ordinal filter. (b) EER of dilobe ordinal filter. (c) DI of trilobe ordinal filter. (d) EER of trilobe ordinal filter.

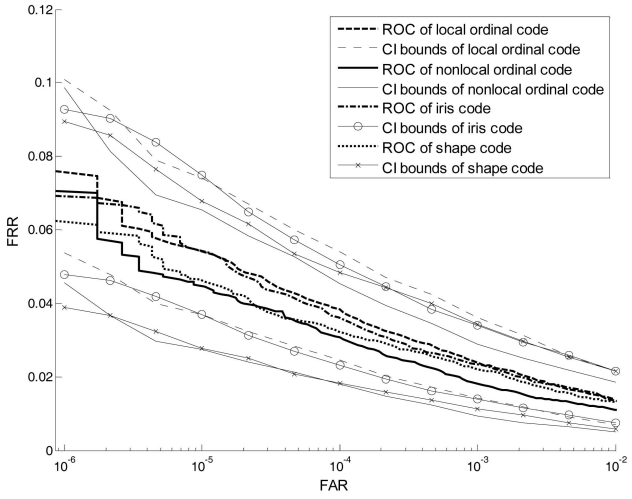

Fig. 23. ROC curves of iris recognition algorithms based on ICE2005-Left database.

5.4 Remarks

Although the UBath, CASIA, and ICE iris image databases are different in sensors and subjects, a number of consistent conclusions can be drawn from the experimental results with these databases.

TABLE 4
Comparison of Recognition Performance on ICE2005-Left Iris Database

Method	EER	DI	Template (Bytes)	Time (ms)
Di-lobe OC (d=5)	1.35×10^{-2}	3.93	128	5.2
Di-lobe OC (d=9)	1.24×10^{-2}	4.18	128	5.2
Di-lobe OC (d=5 plus d=9)	1.13×10^{-2}	4.13	256	10.4
Tri-lobe OC (d=5)	2.65×10^{-2}	3.34	128	5.2
Tri-lobe OC (d=11)	1.31×10^{-2}	4.19	128	5.2
Tri-lobe OC (d=5 plus d=11)	1.19×10^{-2}	3.97	256	10.4
Local OC (Di-lobe d=5 plus Tri-lobe d=5)	1.22×10^{-2}	3.74	256	10.4
Non-local OC (Di-lobe d=9 plus Tri-lobe d=11)	1.06×10^{-2}	4.26	256	10.4
Iris code [1]	1.27×10^{-2}	3.82	256	35.2
Shape code [6]	1.23×10^{-2}	4.25	256	29.6
Multi-scale OC (5×5 :Di-lobe d=9 plus Tri-lobe d=5; 9×9 :Di-lobe d=12 plus Tri-lobe d=9)	6.32×10^{-3}	4.56	2368	96.2

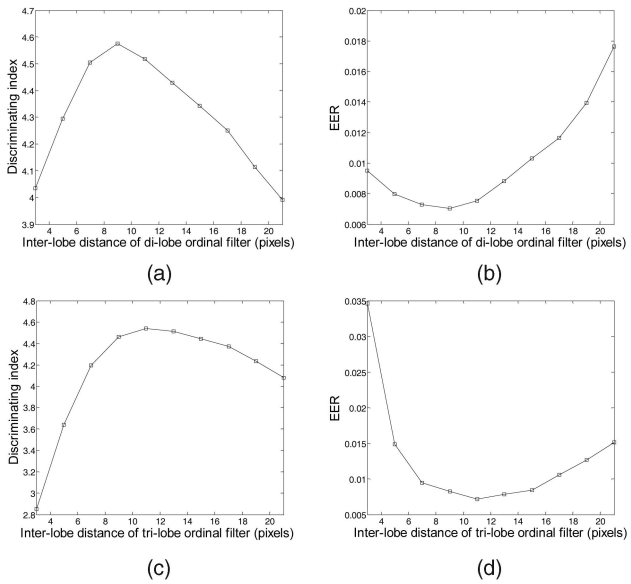

Fig. 24. Performance of ordinal filter as a function of interlobe distance on ICE2005-Right database. (a) DI of dilobe ordinal filter. (b) EER of dilobe ordinal filter. (c) DI of trilobe ordinal filter. (d) EER of trilobe ordinal filter.

- Ordinal feature representation appears to be the common factor to the success of the state-of-the-art iris recognition algorithms. They all achieve good performance in evaluation (i.e., high accuracy, fast processing, and compact templates).
- Ordinal measures are a general image analysis method and differences in ordinal filters result in the difference of recognition results.
- In general, increasing the interlobe (or interregion) distance makes ordinal measures more effective in iris recognition. Nonlocal ordinal measures are superior to local ones since neighboring image regions are highly redundant in information and long-distance comparison has higher contrast magnitude so as to improve the robustness of ordinal codes. However, if the image regions involved in ordinal comparison are too far from each other, the performance of ordinal measures may degrade due to occlusions and nonuniform illumination. So, the trade-off is that an intermediate interregion distance should be chosen in ordinal feature extraction. A simple rule learned from the experiences is that the interlobe distance should be twice the basic lobe's diameter to achieve optimal results.

TABLE 5
Comparison of Recognition Performance on ICE2005-Right Iris Database

Method	EER	DI	Template (Bytes)	Time (ms)
Di-lobe OC (d=5)	7.99×10^{-3}	4.30	128	5.2
Di-lobe OC (d=9)	7.05×10^{-3}	4.57	128	5.2
Di-lobe OC (d=5 plus d=9)	6.19×10^{-3}	4.52	256	10.4
Tri-lobe OC (d=5)	1.49×10^{-2}	3.64	128	5.2
Tri-lobe OC (d=11)	7.14×10^{-3}	4.54	128	5.2
Tri-lobe OC (d=5 plus d=11)	6.05×10^{-3}	4.30	256	10.4
Local OC (Di-lobe d=5 plus Tri-lobe d=5)	7.18×10^{-3}	4.08	256	10.4
Non-local OC (Di-lobe d=9 plus Tri-lobe d=11)	5.72×10^{-3}	4.64	256	10.4
Iris code [1]	7.96×10^{-3}	4.22	256	35.2
Shape code [6]	5.84×10^{-3}	4.63	256	29.6
Multi-scale OC (5×5 :Di-lobe d=9 plus Tri-lobe d=5; 9×9 :Di-lobe d=12 plus Tri-lobe d=9)	4.68×10^{-3}	5.02	2368	96.2

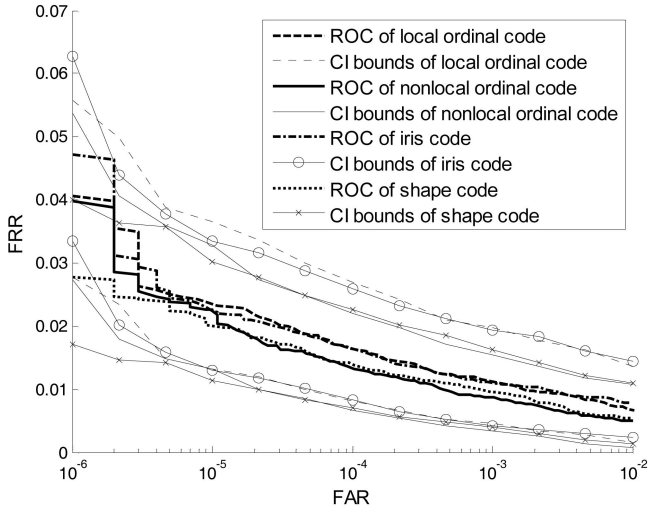

Fig. 25. ROC curves of iris recognition algorithms on ICE2005-Right database.

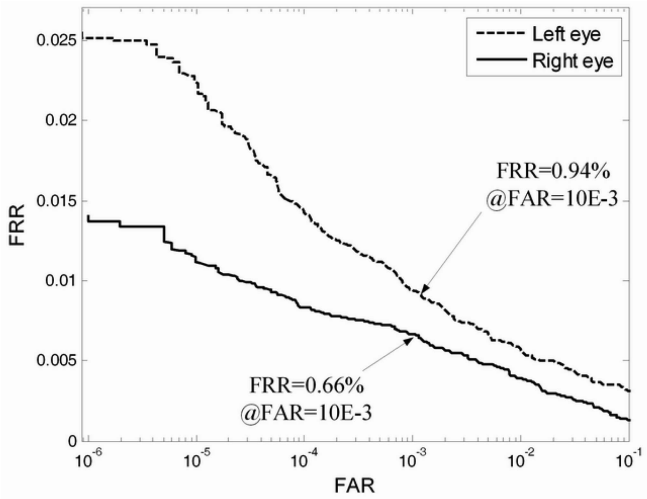

Fig. 26. ROC curves of multiscale ordinal measures on the ICE2005 database.

- The computation of ordinal measures can be simplified to additions and subtractions only, which facilitates the realization of iris recognition algorithms via hardware and makes real-time iris recognition possible in embedded systems such as PDAs and cell phones.
- Ordinal measures with different parameters are complementary to each other. So, information fusion of ordinal filters with different intra and interlobe parameters such as scale, shape, orientation, distance, and measurements (such as intensity, energy, contrast, and some well-developed texture features) can further improve the accuracy of iris recognition.
- Because existing iris recognition methods are almost all limited to local image filtering (i.e., exhibitory and inhibitory lobes are very close to each other), the ordinal measures based on nonlocal differential filters break this limitation and illustrate the promising direction to improve iris recognition performance.

6 Discussions and Conclusions

In this paper, a novel and general framework for iris feature representation and recognition has been presented. The framework is based on ordinal measures, a theoretically simple but practically very powerful feature model. The major contributions of this paper include:

1. The results of this study demonstrate that ordinal measures are informative and robust features for iris recognition despite its simplicity. Our work has shown that ordinal features can be powerful enough for complex tasks such as personal identification, contrary to some views [31].
2. Since the state-of-the-art iris recognition methods can be interpreted in the framework of ordinal measures, it is possible to develop an iris feature model based on ordinal measures as a standard iris feature format. Such a compact representation of iris features is helpful for widespread applications of iris recognition in the storage, transmission, and identification process.
3. The results obtained from this novel approach provide better insight into why some best performing state-of-the-art iris recognition algorithms can work successfully. Our results help to explain why the iris pattern is so discriminative, and provide useful information for the investigation into the individuality and discriminability of iris biometrics.
4. Compared with local ordinal measures, nonlocal ordinal measures, in general, perform better. The work in this paper greatly enriches the previous general framework of iris recognition from local comparisons [39] to nonlocal comparisons [40] because the local ordinal relationships are the special cases of nonlocal comparisons.
5. With the guidance of this novel feature representation model, new and improved iris recognition systems may be developed by different parameter settings of ordinal filters.
6. Due to the easy implementation of ordinal measures, fast algorithms of iris recognition can be developed for embedded systems such as mobile phones, PDAs, and digital cameras.
7. Although the method based on ordinal measures is developed in the context of iris recognition, we think that this is a general scheme for image representation applicable to many other detection or recognition tasks.

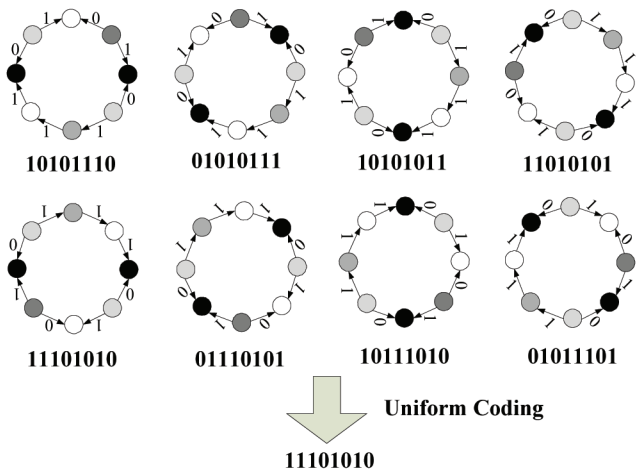

Fig. 27. Rotation invariant ordinal feature coding scheme.

Although promising results have been obtained in this paper, there are many open questions deserving further investigation:

- *Theoretic basis of ordinal measures*. This paper only provides a simple analysis of some basic properties of ordinal measures. Mathematical models may be adopted to better define and analyze ordinal measures. For example, nonparametric robust statistics (e.g., the concepts of order statistics, rank statistics, Wilcoxon rank sum, break points, etc.) can be introduced to establish the theoretic basis of ordinal measures.
- *Novel image features based on ordinal measures.* Novel image descriptors can be proposed in the framework of ordinal measures. Ordinal measures may be combined with other image operators to achieve some desirable properties in image representation, such as scale invariance, rotation invariance, affine invariance, and robustness against deformation. For example, rotation invariant ordinal coding may be achieved by transforming all circular ordinal measures into a uniform code (see Fig. 27).
- *Ordinal feature selection*. Flexibility of parameters in ordinal measures results in an extremely huge feature set. Of course, different ordinal features have different distinctiveness and robustness for visual recognition. Moreover, correlation between different ordinal measures causes the redundancy of information in feature representation. So, machine learning methods such as boosting can be used to select the optimal ordinal feature set from the massive vocabulary.
- *Fusion of ordinal measures and higher level image measures*. Nominal, ordinal, interval, and ratio measures describe image contents from different scales.

Although ordinal measures are robust, they lose some magnitude information which may be useful for visual recognition. So, it is expected to obtain a more powerful image representation by combining ordinal measures with higher level image measures such as interval measures. However, information fusion of cross-level image measurements is a relatively new and challenging research issue. We plan to train object recognition classifier with a cascaded structure so that ordinal measures and higher level measures may be used at multiple stages to achieve a coarse-to-fine feature representation.

APPENDIX A
INVARIANCE OF ORDINAL MEASURES

According to the Lambertian model, the intensity field of a digital iris image $I(x,y,t)$ at a given time t is jointly determined by illumination $i(x,y,t)$, reflectance $r(x,y)$, and geometry $\alpha(x,y,t)$:

$$I(x,y,t) = i(x,y,t)r(x,y)\cos\alpha(x,y,t). \tag{4}$$

Because the pigment of microstructures in iris has different photometric properties on absorption and reflection of NIR illumination, $r(x,y)$ always varies from region to region and determines the randomness of iris texture. Clearly, the reflectance $r(x,y)$ is the intrinsic property of iris patterns, being both informative and invariant to the external environment. In contrast, both $i(x,y,t)$ and $\alpha(x,y)$ are the extrinsic factors of iris image formation. In order to extract the intrinsic features of iris image for recognition, it is a straightforward idea to estimate the exact value of $r(x,y)$ given the observation $I(x,y,t)$. Then, iris matching could be simplified to compare the reflectance of two iris images from pixel to pixel. However, it is a difficult computer vision problem to reconstruct reflectance from image and almost impossible in real-time iris recognition application. But it is fortunate that we can estimate ordinal measures of reflectance instead of intrinsic iris feature representation.

Suppose the reflectance coefficients of two iris image regions are $r(x,y)$ and $r(x+\Delta x, y+\Delta y)$, respectively. Because the iris is physically very small and illuminated at a distance, the illumination strength received by different iris regions is expected to be approximately identical. As iris surface is piecewise smooth, the surface normal of neighboring iris regions should also be approximately identical. So, given small Δx and Δy, we have

$$i(x+\Delta x, y+\Delta y, t) \approx i(x,y,t) \tag{5}$$

and

$$\alpha(x+\Delta x, y+\Delta y, t) \approx \alpha(x,y,t), \tag{6}$$

so

$$\frac{r(x,y)}{r(x+\Delta x, y+\Delta y)} \approx \frac{I(x,y,t)}{I(x+\Delta x, y+\Delta y, t)}. \tag{7}$$

From the above equations, it is reasonable (at least for most cases) to derive that

$$\begin{aligned} r(x,y) &\gtrless r(x+\Delta x, y+\Delta y) \\ &\Leftrightarrow I(x,y,t) \gtrless I(x+\Delta x, y+\Delta y, t). \end{aligned} \tag{8}$$

Equation (8) means that ordinal measures of reflectance can be estimated from ordinal intensity relationship between the corresponding image regions. Moreover, such an ordinal relation is stable across multiple sessions of iris image acquisition. In ideal situation (without noise), the corresponding ordinal measures of within-class iris images should be identical:

$$\begin{aligned} \frac{r(x,y)}{r(x+\Delta x, y+\Delta y)} &= \frac{I(x,y,t_1)}{I(x+\Delta x, y+\Delta y, t_1)} \\ &= \cdots\cdots = \frac{I(x,y,t_{\mathrm{n}})}{I(x+\Delta x, y+\Delta y, t_{\mathrm{n}})}. \end{aligned} \tag{9}$$

So, for intraclass iris images captured at different sessions t_1 and t_2,

$$\begin{aligned} I(x,y,t_1) &\gtrless I(x+\Delta x, y+\Delta y, t_1) \Leftrightarrow \\ I(x,y,t_2) &\gtrless I(x+\Delta x, y+\Delta y, t_2). \end{aligned} \tag{10}$$

Equation (10) illustrates the core idea of ordinal-measures-based iris recognition method, establishing an individual's identity by comparing the ordinal measures of his iris image with that of a template. It is assumed that ordinal measures of intraclass iris images should be largely matched. In contrast, ordinal measures of interclass iris images have no intrinsic correlation, so their match rate is only around 50 percent.

Of course, ordinal measures of iris images are not limited to pixel intensity values. The values used for ordinal comparison may be the results of image transformation or the weighted intensity of a group of pixels. For example, we can derive a series of ordinal measures from (8):

$$\begin{aligned} r(x,y) &\gtrless r(x+\Delta x, y+\Delta y) \\ &\Rightarrow f(r(x,y)) \gtrless f(r(x+\Delta x, y+\Delta y)) \\ &\Rightarrow f(I(x,y,t)) \gtrless f(I(x+\Delta x, y+\Delta y, t)), \end{aligned} \tag{11}$$

$$\begin{aligned} &w_1 I(x_1,y_1) + w_2 I(x_2,y_2) < w_3 I(x_3,y_3) + w_4 I(x_4,y_4) \\ &\quad\Rightarrow w_1 r(x_1,y_1) + w_2 r(x_2,y_2) < w_3 r(x_3,y_3) + w_4 r(x_4,y_4), \end{aligned} \tag{12}$$

where f(x) is a monotonic increasing function, w_i $(i = 1,2,3,4)$ are the positive coefficients, and (x_i, y_i) $(i = 1,2,3,4)$ are the spatial locations of the image region. Equation (11) indicates that ordinal measures of iris image are inherently illumination insensitive and stable to any monotonic or linear intensity transform, like Gamma correction and gain difference between sensors. Ordinal measures across image regions are also robust against misalignment and nonlinear deformation to some extent due to the local similarity property of image pixels. Because the ordinal measures of iris images are determined by the physical properties of iris physiological structures, they are expected to be invariant to sensor differences.

It should be noted that the above derivations are not so strict and only hold for most of iris image regions under normal imaging conditions. In particular, relief features (e.g., a raised bump or ridges, versus a depressed crypt in

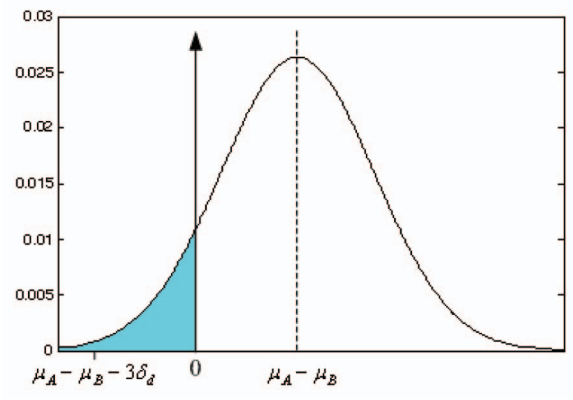

Fig. 28. The probability of ordinal code flipping because of additive Gaussian noise.

the iris) may yield different ordinal measures when the angle of illumination is changed, from one side to the other. In addition, abnormal illumination settings may break the conclusions. For example, when iris is illuminated with nonuniform structured lighting, the received photons may be largely different between neighboring iris regions. Then, the ordinal measures of the iris image regions may not be equal to the ordinal relations of their reflectance. Nevertheless, iris recognition is determined by a large number of ordinal measures, so these exceptions usually cannot change the decision results.

APPENDIX B
ROBUSTNESS OF ORDINAL MEASURES

Here, ordinal measure is defined as the qualitative relationship between the average intensity of two iris image regions (A and B). Each region includes K pixels and the intensity of each pixel is assumed to follow an independent and identical Gaussian distribution. Suppose $A \sim (\mu_A, \delta^2), B \sim (\mu_B, \delta^2)$, and the average intensity difference $I_d = \mu_A - \mu_B > 0$. If there is additive Gaussian noise N in iris image and $N \sim (\mu_N, \delta_N^2)$, so region $A' \sim (\mu_A + \mu_N, \delta^2 + \delta_N^2)$ and average intensity of region $A' I_{A'} \sim (\mu_A + \mu_N, (\delta^2 + \delta_N^2)/K)$; region $B' \sim (\mu_B + \mu_N, \delta^2 + \delta_N^2)$, and average intensity of region $B' I_{B'} \sim (\mu_B + \mu_N, (\delta^2 + \delta_N^2)/K)$. Then, the average intensity difference between A' and B' is $I_{d'} = I_{A'} - I_{B'} \sim (\mu_A - \mu_B, (2\delta^2 + 2\delta_N^2)/K)$. So, the probability of flipping the ordinal code between regions A and B because of noise is

$$P\{\mathrm{OM}(A,B) \neq \mathrm{OM}(A',B')\} = P\{I_{d'} < 0\} = \int_{-255}^{0} \frac{1}{\sqrt{2\pi}\delta_d} e^{-[x-(\mu_A-\mu_B)]^2/2\delta_d^2} dx, \quad (13)$$

where

$$\delta_d = \sqrt{(2\delta^2 + 2\delta_N^2)/K}. \quad (14)$$

The probability of OM flipping is also illustrated as the shaded area in Fig. 28. From (13) and Fig. 28, we can draw two conclusions:

- The larger the magnitude difference between two variables involved in ordinal comparison, the more robust their ordinal measures against additive Gaussian noise. For example, higher $\mu_A - \mu_B$ leads to lower $P\{\mathrm{OM}(A,B) \neq \mathrm{OM}(A',B')\}$.
- The larger the image region used for ordinal feature extraction, the more robust the ordinal measures. For example, larger K leads to smaller δ_d, which, in turn, leads to lower $P\{\mathrm{OM}(A,B) \neq \mathrm{OM}(A',B')\}$.

For a typical iris image in practice, the contrast magnitude between two 7×7 image block pairs is 17.36 (the average contrast magnitude of thousands of iris image block pairs with random orientations), and the average standard deviation is 18.11. So, the probability of OM flipping is only 0.04 percent when the signal to noise ratio $\delta^2/\delta_N^2 = 1$ according to (13). Even when $\delta^2/\delta_N^2 = 0.1$, the probability of OM flipping only increases to 7.61 percent. Based on the above analysis, we can see the robustness of ordinal measures against noise.

Although the above analysis is based on the assumption of additive Gaussian noise and independent and identical Gaussian distributions of pixel values, the conclusions we have made are of general value.

ACKNOWLEDGMENTS

The authors are grateful to the anonymous reviewers for their constructive comments and suggestions. They would like to thank the University of Bath and NIST for sharing their iris image databases with us. This work was supported in part by the National Basic Research Program of China (Grant No. 2004CB318110), the Natural Science Foundation of China (Grant No. 60736018, 60702024), and the Hi-Tech Research and Development Program of China (Grant No. 2006AA01Z193, 2007AA01Z162). The work described in this paper has been filed for patents.

REFERENCES

[1] J. Daugman, "High Confidence Visual Recognition of Persons by a Test of Statistical Independence," *IEEE Trans. Pattern Analysis and Machine Intelligence*, vol. 15, no. 11, pp. 1148-1161, Nov. 1993.
[2] J. Daugman, "Statistical Richness of Visual Phase Information: Update on Recognizing Persons by Iris Patterns," *Int'l J. Computer Vision*, vol. 45, no. 1, pp. 25-38, 2001.
[3] R.P. Wildes, J.C. Asmuth, G.L. Green, S.C. Hsu, R.J. Kolczynski, J.R. Matey, and S.E. McBride, "A Machine-Vision System for Iris Recognition," *Machine Vision and Applications*, vol. 9, pp. 1-8, 1996.
[4] W.W. Boles and B. Boashash, "A Human Identification Technique Using Images of the Iris and Wavelet Transform," *IEEE Trans. Signal Processing*, vol. 46, no. 4, pp. 1185-1188, Apr. 1998.
[5] L. Ma, T. Tan, Y. Wang, and D. Zhang, "Personal Identification Based on Iris Texture Analysis," *IEEE Trans. Pattern Analysis and Machine Intelligence*, vol. 25, no. 12, pp. 1519-1533, Dec. 2003.
[6] L. Ma, T. Tan, Y. Wang, and D. Zhang, "Efficient Iris Recognition by Characterizing Key Local Variations," *IEEE Trans. Image Processing*, vol. 13, no. 6, pp. 739-750, June 2004.
[7] C. Tisse, L. Martin, L. Torres, and M. Robert, "Person Identification Technique Using Human Iris Recognition," *Proc. Int'l Conf. Vision Interface*, pp. 294-299, 2002.
[8] J. Huang, L. Ma, Y. Wang, and T. Tan, "Iris Recognition Based on Local Orientation Description," *Proc. Sixth Asian Conf. Computer Vision*, vol. 2, pp. 954-959, 2004.
[9] S. Noh, K. Bae, and J. Kim, "A Novel Method to Extract Features for Iris Recognition System," *Proc. Fourth Int'l Conf. Audio- and Video-Based Biometric Person Authentication*, pp. 838-844, 2003.

[10] C. Sanchez-Avila and R. Sanchez-Reillo, "Two Different Approaches for Iris Recognition Using Gabor Filters and Multiscale Zero-Crossing Representation," *Pattern Recognition,* vol. 38, no. 2, pp. 231-240, 2005.
[11] C. Park, J. Lee, M. Smith, and K. Park, "Iris-Based Personal Authentication Using a Normalized Directional Energy Feature," *Proc. Fourth Int'l Conf. Audio- and Video-Based Biometric Person Authentication,* pp. 224-232, 2003.
[12] S. Lim, K. Lee, O. Byeon, and T. Kim, "Efficient Iris Recognition through Improvement of Feature Vector and Classifier," *ETRI J.,* vol. 23, no. 2, pp. 61-70, 2001.
[13] J. Thornton, M. Savvides, and V. Kumar, "A Bayesian Approach to Deformed Pattern Matching of Iris Images," *IEEE Trans. Pattern Analysis and Machine Intelligence,* vol. 29, no. 4, pp. 596-606, Apr. 2007.
[14] L. Ma, T. Tan, D. Zhang, and Y. Wang, "Local Intensity Variation Analysis for Iris Recognition," *Pattern Recognition,* vol. 37, no. 6, pp. 1287-1298, 2004.
[15] J. Cui, Y. Wang, T. Tan, L. Ma, and Z. Sun, "An Iris Recognition Algorithm Using Local Extreme Points," *Proc. First Int'l Conf. Biometric Authentication,* pp. 442-449, 2004.
[16] D.M. Monro, S. Rakshit, and D. Zhang, "DCT-Based Iris Recognition," *IEEE Trans. Pattern Analysis and Machine Intelligence,* vol. 29, no. 4, pp. 586-595, Apr. 2007.
[17] Z. Sun, Y. Wang, T. Tan, and J. Cui, "Robust Direction Estimation of Gradient Vector Field for Iris Recognition," *Proc. 17th Int'l Conf. Pattern Recognition,* vol. 2, pp. 783-786, 2004.
[18] Int'l Biometrics Group, "Independent Testing of Iris Recognition Technology,"Final Report, http://www.biometricgroup.com/reports/public/ITIRT.html, May 2005.
[19] Iris Challenge Evaluation, http://iris.nist.gov/ice/, 2009.
[20] P. Sinha, "Qualitative Representations for Recognition," *Lecture Notes in Computer Science,* vol. 2525, pp. 249-262, 2002.
[21] S. Stevens, "On the Theory of Scales of Measurement," *Science,* vol. 103, no. 2684, pp. 677-680, June 1946.
[22] M. Kendall and J.D. Gibbons, *Rank Correlation Methods,* fifth ed. Edward Arnold, 1990.
[23] G.C. DeAngelis, I. Ohzawa, and R.D. Freeman, "Spatiotemporal Organization of Simple-Cell Receptive Fields in the Cat's Striate Cortex. I. General Characteristics and Postnatal Development," *J. Neurophysiology,* vol. 69, no. 4, pp. 1091-1117, 1993.
[24] R. Van Rullen and S.J. Thorpe, "Rate Coding versus Temporal Order Coding: What the Retinal Ganglion Cells Tell the Visual Cortex," *Neural Computation,* vol. 13, no. 6, pp. 1255-1283, 2001.
[25] P. Sinha, "Perceiving and Recognizing Three-Dimensional Forms," PhD dissertation, Massachusetts Inst. of Technology, pp. 141-165, 1995.
[26] P. Lipson, E. Grimson, and P. Sinha, "Configuration Based Scene Classification and Image Indexing," *Proc. IEEE Conf. Computer Vision and Pattern Recognition,* pp. 1007-1013, June 1997.
[27] D. Bhat and S. Nayar, "Ordinal Measures for Image Correspondence," *IEEE Trans. Pattern Analysis and Machine Intelligence,* vol. 20, no. 4, pp. 415-423, Apr. 1998.
[28] M. Partio, B. Cramariuc, and M. Gabbouj, "Texture Similarity Evaluation Using Ordinal Co-Occurrence," *Proc. IEEE Int'l Conf. Image Processing,* pp. 1537-1540, 2004.
[29] F. Smeraldi "Ranklets: A Complete Family of Multiscale, Orientation Selective Rank Features," Research Report RR0309-01, Dept. of Computer Science, Queen Mary, Univ. of London, Sept. 2003.
[30] J. Sadr, S. Mukherjee, K. Thoresz, and P. Sinha, "The Fidelity of Local Ordinal Encoding," *Advances in Neural Information Processing Systems,* T. Dietterich, S. Becker, and Z. Ghahramani, eds., MIT Press, 2002.
[31] K.J. Thoresz, "Qualitative Representations for Recognition," master's thesis, Massachusetts Inst. of Technology, 2002.
[32] B. Balas and P. Sinha, "Dissociated Dipoles: Image Representation via Non-Local Comparisons," CBCL Paper #229/AI Memo #2003-018, Massachusetts Inst. of Technology, 2003.
[33] B. Balas and P. Sinha, "Receptive Field Structures for Recognition," CBCL Paper #246/AI Memo #2005-006, Massachusetts Inst. of Technology, 2005.
[34] R. Young, R. Lesperance, and W. Meyer, "The Gaussian Derivative Model for Spatial-Temporal Vision: I. Cortical Model," *Spatial Vision,* vol. 14, nos. 3/4, pp. 261-319, 2001.
[35] University of Bath Iris Image Database, http://www.bath.ac.uk/elec-eng/pages/sipg/irisweb/, 2009.
[36] CASIA Iris Image Database, http://www.cbsr.ia.ac.cn/irisdatabase.htm, 2009.
[37] N. Macmillan and C. Creelman, *Detection Theory: A Users Guide.* Cambridge Univ. Press, 1991.
[38] R.M. Bolle, N.K. Ratha, and S. Pankanti, "Error Analysis of Pattern Recognition Systems: The Subsets Bootstrap," *Computer Vision and Image Understanding,* vol. 93, no. 1, pp. 1-33, 2004.
[39] Z. Sun, T. Tan, and Y. Wang, "Robust Encoding of Local Ordinal Measures: A General Framework of Iris Recognition," *Lecture Notes in Computer Science,* vol. 3087, pp. 270-282, 2004.
[40] Z. Sun, T. Tan, and Y. Wang, "Iris Recognition Based on Non-Local Comparisons," *Lecture Notes in Computer Science,* vol. 3338, pp. 67-77, 2004.
[41] P.J. Phillips, K.W. Bowyer, and P.J. Flynn, "Comments on the CASIA Version 1.0 Iris Data Set," *IEEE Trans. Pattern Analysis Machine Intelligence,* vol. 29, no. 10, pp. 1869-1870, Oct. 2007.
[42] ISO/IEC 19794-6: 2005 Information technology—Biometric Data Interchange Formats—Part 6: Iris Image Data, 2005.

Zhenan Sun received the BE degree in industrial automation from Dalian University of Technology in 1999, the MS degree in system engineering from Huazhong University of Science and Technology in 2002, and the PhD degree in pattern recognition and intelligent systems from CASIA in 2006. He is an associate professor in the Institute of Automation, Chinese Academy of Sciences (CASIA). In March 2006, he joined the Center of Biometrics and Security Research (CBSR) in the National Laboratory of Pattern Recognition (NLPR) of CASIA as a faculty member. He is a member of the IEEE and the IEEE Computer Society. His current research focuses on biometrics, pattern recognition, and computer vision.

Tieniu Tan received the BSc degree in electronic engineering from Xi'an Jiaotong University, China, in 1984, and the MSc and PhD degrees in electronic engineering from Imperial College of Science, Technology and Medicine, London, United Kingdom, in 1986 and 1989, respectively. In October 1989, he joined the Computational Vision Group in the Department of Computer Science, The University of Reading, United Kingdom, where he worked as a research fellow, a senior research fellow, and a lecturer. In January 1998, he returned to China to join the National Laboratory of Pattern Recognition (NLPR), Institute of Automation of the Chinese Academy of Sciences (CAS), Beijing, China, where he is currently a professor and the director of the NLPR, and a former director general of the Institute (2000-2007). He is also a deputy secretary general of the CAS and the head of the Department of Automation, The University of Science and Technology of China (USTC). He has published more than 290 research papers in refereed journals and conferences in the areas of image processing, computer vision, and pattern recognition. His current research interests include biometrics, image and video understanding, information hiding, and information forensics. He is a fellow of the IEEE and the International Association of Pattern Recognition (IAPR). He has served as the chair or a program committee member for many major national and international conferences. He is or once served as an associate editor or a member of the editorial board of many leading international journals including the *IEEE Transactions on Pattern Analysis and Machine Intelligence (TPAMI)*, *IEEE Transactions on Automation Science and Engineering*, *IEEE Transactions on Information Forensics and Security*, *IEEE Transactions on Circuits and Systems for Video Technology*, *Pattern Recognition*, *Pattern Recognition Letters*, *Image and Vision Computing*, etc. He is the editor-in-chief of the *International Journal of Automation and Computing* and *Acta Automatica Sinica*. He is the chair of the IAPR Technical Committee on Biometrics, the founding chair of the IAPR/IEEE International Conference on Biometrics (ICB) and the IEEE International Workshop on Visual Surveillance. He currently serves as the executive vice president of the Chinese Society of Image and Graphics, and the deputy president of the Chinese Automation Association.